

Dynamical manifestation of an evolving Berry phase as a frequency shift of the resonance transition between two eigenstates

Koichi Toriyama, Akihide Oguchi, and Atsuo Morinaga*

Faculty of Science and Technology, Tokyo University of Science, 2641 Yamazaki, Noda-shi, Chiba 278-8510, Japan

(Received 29 July 2011; published 2 December 2011)

We investigate the phenomenon that a Berry phase evolving linearly in time induces a frequency shift of the resonance transition between two eigenstates, regardless of whether or not they are superposed. Using the magnetic-field-insensitive two-photon microwave—radio-frequency transition, which is free of any other dynamical frequency shift, we demonstrate that the frequency shift caused by a uniform rotation of the magnetic field corresponds to the derivative of the Berry phase with respect to time and depends on the direction of rotation of the magnetic field.

DOI: [10.1103/PhysRevA.84.062103](https://doi.org/10.1103/PhysRevA.84.062103)

PACS number(s): 03.65.Vf, 06.20.F–, 32.30.Bv, 32.60.+i

I. INTRODUCTION

Since Berry predicted in 1984 that, in a cyclic adiabatic process, one in which the slowly time-varying Hamiltonian returns to its original form via a circuit C , a quantum state may acquire a “geometrical” phase factor $\exp[-im\Omega(C)]$, where m is the spin component and Ω is the solid angle, in addition to the normal “dynamical” phase factor $\exp[-(i/\hbar)\int E_m(t)dt]$ [1], where $E_m(t)$ is the energy of a state m , many experimental identifications of the Berry phase have been carried out in various fields of physics [2]. However, these experiments often encountered the problem of separating the geometric phase from a much larger dynamical phase. To observe a clean geometric phase, the dynamical phase component needs to be minimized or eliminated in experimental methods [3], or the nonadiabatic evolution proposed by Aharanov and Anandan should be used [4], which has enabled the experimental separation of geometric and dynamical phases [5]. Recently, we have used magnetic-field-insensitive two-photon “clock” transitions, where the sign of the g factor is reversed for the upper and lower states [6], and clearly found a dependence of the Berry phase on the sign of the g factor [7]. When the direction of the quantized magnetic field and the sense of the rotation are defined, the solid angle Ω is $2\pi(1-\cos\theta)$ or $-2\pi(1+\cos\theta)$ depending on the sign of the g factor.

In 1988, Simon *et al.* considered another interesting situation wherein an evolving nondynamical geometrical phase induces a shift of laser frequency [8]. They confirmed their idea using an optical experiment where the polarization of a laser beam is rotated continuously on the Poincaré sphere. Such evolving Berry phases were also suggested by Moody *et al.* in nuclear magnetic resonance (NMR) [9], and demonstrated as both an adiabatic rotational splitting of the nuclear quadrupole resonance (NQR) in the free-induction decay signals from a rotating sample by Tycko [10] and Fourier-transform NMR spectra under a continuously rotating radio-frequency field by Suter *et al.* [11]. In the above experiments, a superposition state of two eigenstates is created at first and acquires a relative phase difference during the rotation.

These previous studies predict that a Berry phase evolving linearly in time induces a shift of the transition frequency

between two eigenstates. However, to the best of our knowledge, there has been no report that shows such a dynamical manifestation of the Berry phase as a shift of the transition frequency between two eigenstates. In this paper, we demonstrate that an evolving Berry phase induces a frequency shift of the resonance transition, using the magnetic-field-insensitive two-photon microwave—radio-frequency (MW-rf) transition, which is free of any other dynamical frequency shift.

II. PRINCIPLE AND METHOD

First, we derive the frequency difference between two eigenstates under an action that includes the dynamical phase when the magnetic field B rotates with a semiangle of θ from a rotation axis and a constant rotation speed of $\dot{\phi}$. The Berry phase of the state $|F, m\rangle$ is calculated using a path integral [12],

$$i\langle F, m | \partial_t | F, m \rangle = m\dot{\phi} \cos\theta. \quad (1)$$

Then, the time derivative of the action S is given by

$$\dot{S}_{|F, m\rangle} = -E_{|F, m\rangle} - g_F \mu_B m B + m\hbar\dot{\phi} \cos\theta, \quad (2)$$

where the first term is the eigenenergy of $|F, m\rangle$ and the second term is the Zeeman energy. Therefore, the frequency difference between the lower state $|F, m\rangle$ and the upper state $|F', m'\rangle$ is given by

$$\nu = \hbar^{-1}(E_{|F', m'\rangle} - E_{|F, m\rangle}) + \hbar^{-1}(g_{F'} m' - g_F m) \mu_B B - (2\pi)^{-1}(m' - m)\dot{\phi} \cos\theta. \quad (3)$$

To measure the frequency shift, we used three two-photon MW-rf transitions between ground hyperfine levels of sodium atoms that are insensitive to the magnetic field to the first order and are called clock transitions [7]. Figure 1 shows the energy diagram of the ground-state hyperfine levels of ^{23}Na , with the Zeeman splitting according to the strength of the magnetic field and the three transitions. The g factors of the $F = 1$ and $F = 2$ states are $-1/2$ and $1/2$, respectively. According to the Breit-Rabi equation [13], the resonance frequency $\nu_{-1,1}$ between the $|F = 1, m_F = -1\rangle$ and $|F = 2, m_F = 1\rangle$ states is minimum at $B_0 = 67.7 \mu\text{T}$, which is called the “magic” magnetic field, and it is 762.3 Hz lower than the resonance frequency $\nu_0 = 1.771\,626\,129 \times 10^9$ Hz between the $F = 1$

*morinaga@ph.noda.tus.ac.jp

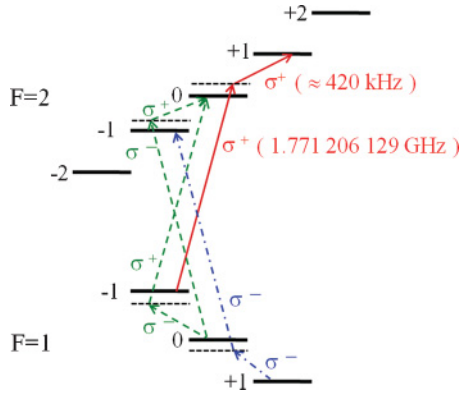


FIG. 1. (Color online) Diagram of the sodium ground hyperfine levels under the magic magnetic field of $67.7 \mu\text{T}$, together with magnetic-field-insensitive two-photon microwave-radiofrequency transitions. Frequency splitting between the magnetic sublevels is 474 kHz .

and $F = 2$ states at zero magnetic field [14]. On the other hand, at a strength of the magnetic field B (in units of μT) around the magic value, the resonance frequency $\nu_{0,0}$ between the $|1,0\rangle$ and $|2,0\rangle$ states is given by $\nu_0 + 0.2218B^2 \text{ Hz}$, and the resonance frequency $\nu_{1,-1}$ between the $|1,1\rangle$ and $|2,-1\rangle$ states is given by $\nu_0 - 762.3 + 0.1664(B + B_0)^2 \text{ Hz}$.

We use two-photon MW-rf excitations to drive these three transitions, as shown in Fig. 1. At the magic magnetic field, the Zeeman splitting frequency is 474 kHz . We apply a pulse of microwave radiation, whose frequency is 420 kHz less than that corresponding to the ground-state hyperfine splitting of Na, namely, ν_0 , along with an rf magnetic field of approximately 420 kHz . This connects the $|1,-1\rangle$ state to the $|2,1\rangle$ state via an intermediate virtual state with detuning of 54 kHz from the $|2,0\rangle$ state by $\sigma^+ - \sigma^+$ polarized fields [15]. Other two-photon excitations are also shown in Fig. 1. A dipole antenna, which generates MWs with a frequency of $1.771\,206\,129 \text{ GHz}$, was set parallel to the x direction near the magneto-optical trap (MOT); thus, the polarization direction of the MWs is perpendicular to the quantization magnetic field (σ polarization). An rf field was produced by a loop antenna near the MOT and swept at a frequency of approximately 420 kHz . To resolve the three magnetic-field-insensitive transitions separated by about a $1\text{--}2 \text{ kHz}$, the widths of these MW and rf pulses were set to $2\text{--}4 \text{ ms}$, and their field strengths were optimized to maximize the strength of the two-photon spectra.

III. EXPERIMENT

The experimental setup used in this experiment was the same as that described in a previous paper [7]. The timing diagram of the present experiment is shown in Fig. 2. Sodium atoms were trapped in a dual-operated MOT [16] and cooled by polarization gradient cooling. The temperature of the sodium atoms was approximately $200 \mu\text{K}$ and the number of trapped atoms was 10^9 with a peak density of $10^{11} \text{ atoms/cm}^3$.

A few milliseconds after the release of atoms from the trap, a magnetic field B_x was applied in the x direction. All the atoms were initialized to the $F = 1$ state by optical pumping. The three magnetic sublevels of the $|1,1\rangle$, $|1,0\rangle$, and $|1,-1\rangle$ states

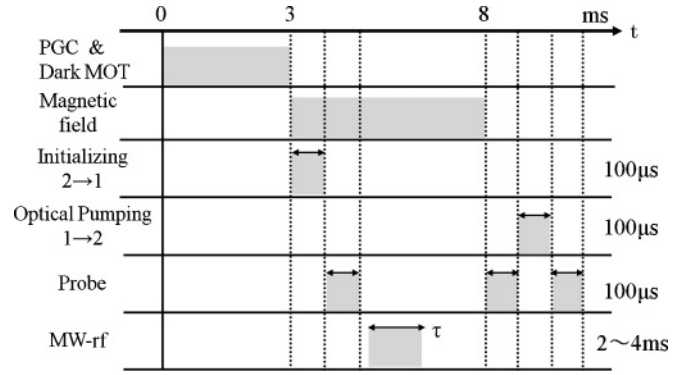


FIG. 2. Timing diagram of measurement. PGC, polarization gradient cooling; MOT, magneto-optical trap. Initializing: all atoms are populated to the $F = 1$ state. Optical pumping: all atoms in the $F = 1$ state are excited to the $F = 2$ state. Probe: the number of atoms populated in the $F = 2$ states is probed. MW-rf: two-photon microwave-radio-frequency pulse with a pulse width of τ .

were populated with equal population probabilities. Next, a magnetic field B_z was applied in the z direction. The resultant magnetic field B was $B = \sqrt{B_x^2 + B_z^2}$ and the semiangle θ from the z axis was $\cos \theta = B_z / \sqrt{B_x^2 + B_z^2}$. In this experiment, B_x was fixed to a magic magnetic field of $67.6 \pm 0.1 \mu\text{T}$, which corresponds to a Larmor frequency of 470 kHz . B_x was adiabatically rotated in the x - y plane with a frequency f (or a period of $T = 1/f$). Magnetic fields along the x and y axes were produced by two mutually orthogonal Helmholtz coils [17]. The coils were driven by alternating currents with a relative phase shift of 90° . During the rotation, the amplitude of each alternating current was adjusted so that the Zeeman-frequency shifts of the resonance for magnetic-field-sensitive transitions were $67.5 \pm 0.4 \mu\text{T}$. The rotation frequency of 200 or 500 Hz used in this study was sufficient to satisfy the adiabatic condition. To change the semiangle θ from the z axis, the magnetic field B_z parallel to the z axis was changed. The strength of B_z was changed from 0 to $\pm 40 \mu\text{T}$, which corresponds to a change of the semiangle from $\pi/3$ to $2\pi/3$. The resultant magnetic field at $\pi/3$ and $2\pi/3$ was 1.15 times larger than that at $\theta = \pi/2$, which yields a frequency shift of at most 17 Hz for the transition between the $|1,-1\rangle$ and $|2,1\rangle$ states. Then, the tip of the resultant magnetic field rotated around the z axis with a semiangle θ . There are two senses of rotation. We define the right-handed rotation around the $+z$ axis as the positive sense of rotation and the left-handed rotation around the $+z$ axis as the negative sense of rotation.

During the rotation of the magnetic field, the atoms were irradiated with a short MW-rf pulse and the frequency of the rf pulse was scanned. The probability of excitation from the $F = 1$ to the $F = 2$ state was measured as follows. After initializing the atoms to the $F = 1$ state, the perfectly transmitted probe intensity I_1 was measured. After the interaction of the atoms with the MW-rf pulse, the probe intensity I_2 transmitted through the atoms in the $F = 2$ state was measured using the same probe light. After application of the optical pumping pulse which excites atoms in the $F = 1$ state to the $F = 2$ state, the probe intensity I_3 transmitted through the total atoms was measured. Then we obtained the excitation probability as $\{\ln(I_1) - \ln(I_2)\} / \{\ln(I_1) - \ln(I_3)\}$.

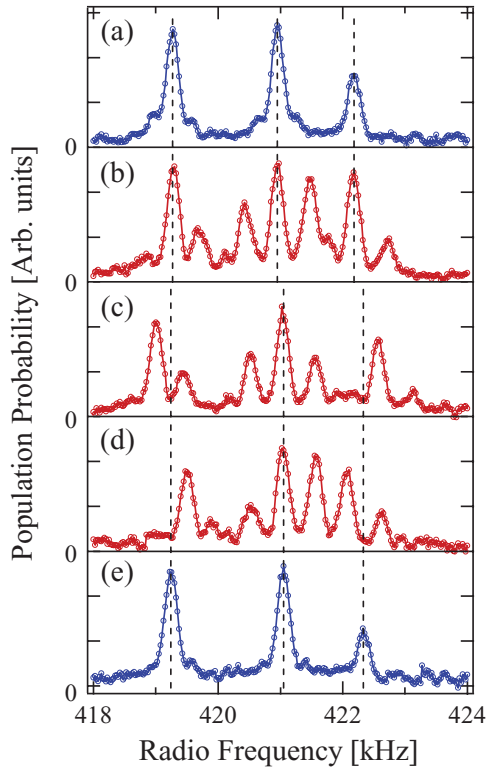


FIG. 3. (Color online) Three spectra of the $|1, -1\rangle \rightarrow |2, 1\rangle$, $|1, 0\rangle \rightarrow |2, 0\rangle$, and $|1, 1\rangle \rightarrow |2, -1\rangle$ two-photon transitions from left to right in each figure. (a) and (b) are the spectra under a magnetic field of $67.7 \mu\text{T}$ at the semiangle of $\theta = \pi/2$. (a) Static magnetic field. (b) Rotating magnetic field at 500 Hz. (c)–(e) are the spectra under a magnetic field of $70.1 \mu\text{T}$. (c) Rotating magnetic field at 500 Hz and $\theta = 5\pi/12$. (d) Rotating magnetic field at 500 Hz and $\theta = 7\pi/12$. (e) Static magnetic field at $\theta = 5\pi/12$.

IV. RESULTS AND DISCUSSION

Figure 3 shows the three spectra of the transition from the $F = 1, m_F = -1$ state to the $F = 2, m_F = 1$ state ($-1 \rightarrow 1$), the transition from the $F = 1, m_F = 0$ state to the $F = 2, m_F = 0$ state ($0 \rightarrow 0$), and the transition from the $F = 1, m_F = 1$ state to the $F = 2, m_F = -1$ state ($1 \rightarrow -1$). Each line has a spectral width of 250 Hz, which corresponds to the reciprocal of the pulse width of two-photon MW-rf excited fields of 4 ms. Figures 3(a) and 3(b) show the spectra under a magnetic field with a strength of $67.7 \mu\text{T}$ and a semiangle of $\theta = \pi/2$, while Figs. 3(c)–3(e) show the spectra under one with a strength of $70.1 \mu\text{T}$ and a semiangle of $\theta = 5\pi/12$ or $7\pi/12$. As shown in Figs. 3(a) and 3(e), under a constant magnetic field, the three spectra are clearly resolved due to the second-order Zeeman effect, but their resonance frequencies in Fig. 3(a) are shifted from those in Fig. 3(e), as indicated by the three dashed lines. The frequency difference for the $1 \rightarrow -1$ line is the largest, but that for the $-1 \rightarrow 1$ line is negligible. Their differences are in good agreement with the values calculated using the Breit-Rabi formula [13].

The spectra in Fig. 3(b) were obtained under a rotating magnetic field with a rotation frequency of 500 Hz and a semiangle of $\theta = \pi/2$. The resonance frequencies for the three lines are the same as those in Fig. 3(a), because there

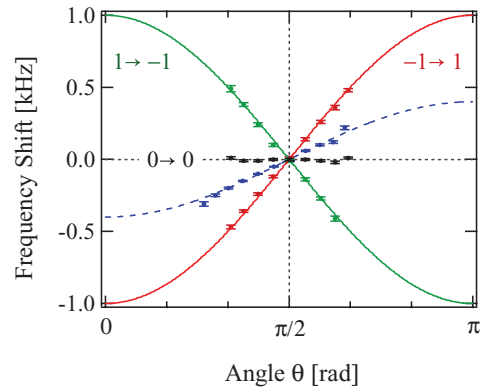


FIG. 4. (Color online) Observed frequency shift as a function of semiangle θ for a right-handed uniform rotation of the magnetic field. $m_F \rightarrow m_{F'}$ represents the $|1, m_F\rangle \rightarrow |2, m_{F'}\rangle$ transition. Data for the $-1 \rightarrow 1$ transition for the rotation frequencies of 500 and 200 Hz are on the solid curve of $-1000\cos\theta$ and on the dashed curve of $-400\cos\theta$, respectively. The data for the $1 \rightarrow -1$ transition for the rotation frequency of 500 Hz are on the curve of $1000\cos\theta$.

is no phase difference due to the Berry phase [7]. We can see clear side resonance peaks on both sides of the resonance peak of the $0 \rightarrow 0$ line. The frequency separation between the center and each side peak is 500 Hz. These side peaks occur owing to the rotation of the magnetic field, as the usual harmonic motion. The spectra in Figs. 3(c) and 3(d) were obtained under a rotating magnetic field with semiangles of $\theta = 7\pi/12$ and $5\pi/12$, respectively. The center frequencies of the $0 \rightarrow 0$ line coincide with that in Fig. 3(e), but in Fig. 3(c) the frequency of the $-1 \rightarrow 1$ line is shifted to the lower-frequency side, while the frequency of the $1 \rightarrow -1$ line is shifted to the higher side. On the other hand, in Fig. 3(d) the relation is reversed. As the frequency of the $-1 \rightarrow 1$ line is not affected by the second-order Zeeman effect, the observed frequency shift should have been induced by the evolving Berry phase.

The frequency shifts of three two-photon MW-rf transitions were measured for various semiangles θ with rotation of the magnetic field at a frequency of $f = 500$ Hz, as shown in Fig. 4. The frequency shift for the $-1 \rightarrow 1$ line varies from negative to positive with an increase in semiangle, while that for the $1 \rightarrow -1$ line varies from positive to negative. Their behaviors are described well using the functions $-2f\cos\theta$ and $2f\cos\theta$, respectively, which are indicated by solid lines. On the other hand, the frequency shift for the $0 \rightarrow 0$ line is constant. These results were observed with an interaction time of 4 ms, which corresponds to twice the period of the rotation frequency. We changed the interaction time to 2 ms, but the frequency shifts were the same as before, although the spectral width broadened to 500 Hz. Next, we changed the rotation frequency to $f = 200$ Hz. Then the MW-rf pulse with a pulse width of 4 ms interacted with atoms for only 0.8 times the period of the rotation. The results for the $-1 \rightarrow 1$ line are also shown in Fig. 4, and they are in good agreement with the function $-2f\cos\theta$, which is indicated by a dashed line. Thus, we checked that these formulas for the frequency shift hold for different frequencies and observation times.

We showed in our previous paper [7] that the Berry phase for the $-1 \rightarrow 1$ line gains a phase of $4\pi\cos\theta$ for a complete rotation

of the magnetic field with a semiangle θ . If the magnetic field rotates at a constant speed with a period of T , namely, frequency $f = 1/T$, the time derivative of the Berry phase is $4\pi\cos\theta/(2\pi T) = 2f\cos\theta$. Using Eq. (3) with $g = -1/2$ for the $F = 1$ state and $g = 1/2$ for the $F = 2$ state, the resonance frequency of the $-1 \rightarrow 1$ line is given by

$$\nu = (E_{|2,1\rangle} - E_{|1,-1\rangle})/h - 2f\cos\theta = \nu_{-1,1} - 2f\cos\theta. \quad (4)$$

Therefore, the experimental results show that the absolute value of the frequency shift is given by the time derivative of the Berry phase, and the frequency shifts to the negative direction when the Berry phase gains a positive value and vice versa. Thus, the present experimental results are well described by the well-known theoretical framework for describing the Berry phase. Therefore, we confirm that the evolving Berry phase induces a frequency shift of the resonance transition. This means that the resonance frequency of the $-1 \rightarrow 1$ line is perturbed by the rotation of the quantized magnetic field, although it is exceedingly insensitive to the

strength of the magnetic field around the magic magnetic field.

V. CONCLUSION

In this paper, we have demonstrated that an evolving Berry phase induces a frequency shift of the resonance transition as a dynamical manifestation. The value of the shift is proportional to the derivative of the Berry phase with respect to time. When the magnetic field rotates around the z axis with a semiangle θ , the frequency shift depends on the rotation frequency, the semiangle θ , and the magnetic quantum number. Thus, the energy of the quantum system can be changed by a geometrical as well as a dynamical potential.

ACKNOWLEDGMENTS

We are indebted to Hiromitsu Imai for his experimental development of the two-photon MW-rf spectroscopy and Kouta Nanri for his experimental assistance.

-
- [1] M. V. Berry, *Proc. R. Soc. London, Ser. A* **392**, 45 (1984).
 - [2] *Geometric Phases in Physics*, edited by A. Shapere and F. Wilczek (World Scientific, Singapore, 1989).
 - [3] A. Tomita and R. Y. Chiao, *Phys. Rev. Lett.* **57**, 937 (1986).
 - [4] Y. Aharonov and J. Anandan, *Phys. Rev. Lett.* **58**, 1593 (1987).
 - [5] A. G. Wagh, V. C. Rakhecha, J. Summhammer, G. Badurek, H. Weinfurter, B. E. Allman, H. Kaiser, K. Hamacher, D. L. Jacobson, and S. A. Werner, *Phys. Rev. Lett.* **78**, 755 (1997).
 - [6] D. M. Harber, H. J. Lewandowski, J. M. McGuirk, and E. A. Cornell, *Phys. Rev. A* **66**, 053616 (2002).
 - [7] A. Morinaga, K. Toriyama, H. Narui, T. Aoki, and H. Imai, *Phys. Rev. A* **83**, 052109 (2011).
 - [8] R. Simon, H. J. Kimble, and E. C. G. Sudarshan, *Phys. Rev. Lett.* **61**, 19 (1988).
 - [9] J. Moody, A. Shapere, and F. Wilczek, *Phys. Rev. Lett.* **56**, 893 (1986).
 - [10] R. Tycko, *Phys. Rev. Lett.* **58**, 2281 (1987).
 - [11] D. Suter, G. C. Chingas, R. A. Harris, and A. Pines, *Mol. Phys.* **61**, 1327 (1987).
 - [12] J. Anandan, *Nature (London)* **360**, 307 (1992).
 - [13] G. Breit and I. I. Rabi, *Phys. Rev.* **38**, 2082 (1931).
 - [14] D. A. Steck, Sodium D Line Data, <http://steck.us/alkalidata>.
 - [15] K. D. Bonin and T. J. McIlrath, *J. Opt. Soc. Am. B* **1**, 52 (1984).
 - [16] H. Tanaka, H. Imai, K. Furuta, Y. Kato, S. Tashiro, M. Abe, R. Tajima, and A. Morinaga, *Jpn. J. Appl. Phys.* **46**, L492 (2007).
 - [17] A. Takahashi, H. Imai, K. Numazaki, and A. Morinaga, *Phys. Rev. A* **80**, 050102(R) (2009).